

Electronic structure near (210) tilt boundaries in nickel

S. Crampin and D. D. Vvedensky

The Blakett Laboratory, Imperial College, London SW7 2BZ, United Kingdom

J. M. MacLaren

Theoretical Division, Los Alamos National Laboratory, Los Alamos, New Mexico 87545

M. E. Eberhart*

Materials Science and Technology Division, Los Alamos National Laboratory, Los Alamos, New Mexico 87545

(Received 20 April 1989)

We report the first self-consistent electronic structure calculations of an isolated $\Sigma 5$ tilt boundary in a transition metal, including the effects of segregants that induce intergranular brittleness. The local densities of states near the grain boundary show narrowed d bands due to reduced coordination, with the full bandwidth restored within three layers. The presence of S segregants at the grain boundary inhibits Ni bonding across the interface, though the effect of the impurities is effectively screened within three layers.

Grain boundaries are important in mediating a number of physical, chemical, and electronic properties of materials, including deformation behavior. They may act as barriers to dislocation motion by limiting the available slip length, thereby strengthening the material. Furthermore, the influence of impurities at grain boundaries that either strengthen or weaken the boundary is a well-known effect that is of evident importance in designing and manufacturing materials with suitable combinations of mechanical properties for, say, high-temperature applications.¹

Systematic studies of grain boundaries in well-characterized prototype systems can play an important role in developing concepts and computational methods that can then be applied to materials of direct technological interest. However, there have been relatively few studies of the electronic structure at metallic grain boundaries that include, for example, a realistic structural representation of the interface. Electronic-structure calculations using small (~ 10 atoms) clusters²⁻⁵ reveal gross trends but suffer from the uncontrolled effects of free boundaries. Pseudopotential total-energy calculations for idealized structural models of Al grain boundaries⁶ have been used to investigate the effects upon cohesion of As segregants. The fracture energy was calculated, where the As impurities were found to increase grain-boundary cohesion. However, no attempt was made to address the effect of variations in local geometry or the influence of other impurities.

Embedded-atom methods^{7,8} have been used to address several aspects of grain-boundary behavior, including structural relaxations that compare favorably with x-ray-diffraction measurements.⁹ However, the determination of the embedding function is quite an onerous task for systems with many distinct atoms, leading often to *ad hoc* prescriptions for interatomic potentials. Indeed, one of the ultimate goals of electronic-structure calculations of the type presented here is the first-principles determination of interatomic interactions for realistic simulations of deformation behavior, including the variation of the po-

tentials with structural and chemical environment. Additionally, the determination of charge densities and local structures will provide a description of grain-boundary characteristics that complements embedded-atom calculations.

In this Rapid Communication we present the first self-consistent calculation of the electronic structure of an isolated $\Sigma 5$ (210) tilt boundary (where Σ indicates the inverse density of coincident sites) in a transition metal that correctly accounts for the embedding in the parent grains. The calculations have been carried out with a layer Korringa-Kohn-Rostoker (LKRR) method, the details of which are reported elsewhere.¹⁰ LKRR theory provides an elegant and efficient solution to the one-electron Schrödinger equation which retains the accuracy of the KKR method while being applicable to systems with two-dimensional periodicity, such as surfaces and interfaces. In carrying out the calculations for the (210) Ni tilt boundary, three features of LKRR theory are worthy of note: the scaling of central-processor-unit (CPU) time with the complexity of the system, the treatment of closely spaced layers, and self-consistency.

The central quantity of interest is the local energy-resolved charge density $\rho(\mathbf{r};E)$, which is related in the usual way to the diagonal components of the Green's function G in the coordinate representation: $\rho(\mathbf{r};E) = -(1/\pi)\text{Im}G(\mathbf{r},\mathbf{r};E)$. The calculation of the self-consistent electronic structure proceeds by calculating G about each atom in a layer embedded in semi-infinite left and right half-spaces. A mixed basis set is used in the calculation of G , with an expansion in spherical waves for intralayer scattering by the muffin-tin potentials as in standard KKR theory,¹¹ and a plane-wave basis for interlayer scattering, as used in theories of low-energy electron diffraction¹² (LEED). This factorization of the scattering events facilitates a realistic treatment of complex interfaces, since the CPU time scales as $\sum_i n_i^3$, rather than as n_i^3 , where n_i is the number of unique atoms in layer i , and $n_i = \sum_i n_i$ is the total number of unique atoms.

The difficulties associated with the close-spaced layers can easily be seen by examining the form of the plane-wave basis functions which couple layers separated by the vector $\mathbf{c} = (c_{\parallel}, c_z)$, where c_{\parallel} and c_z are the separations in the x - y and z directions, respectively. The basis functions that couple the layers are solutions to the Schrödinger equation at energy E and parallel momentum \mathbf{k} . The convergence of this expansion is uniform provided the z component of the interlayer spacing is nonzero, since for large two-dimensional reciprocal-lattice vectors \mathbf{g} we have,¹³ in Hartree atomic units,

$$\langle \mathbf{r} | \mathbf{K}_{\mathbf{g}}^{\pm} \rangle |_{r=c} = \exp\{i(\mathbf{k} + \mathbf{g}) \cdot \mathbf{c}_{\parallel} + i[2E - (\mathbf{k} + \mathbf{g})^2]^{1/2} | c_z \} \\ \rightarrow \exp[i(\mathbf{k} + \mathbf{g}) \cdot \mathbf{c}_{\parallel}] \exp[-g | c_z |]$$

as $g \rightarrow \infty$. Thus, while exponentially convergent, the rate clearly depends on the size of c_z . In systems where c_z is small, such as a grain boundary, many vectors are required to converge the interlayer scattering to a prescribed accuracy.

Two further factors work against the plane-wave basis for close-spaced layers. First, the number of two-dimensional reciprocal-lattice vectors at a given \mathbf{g} grows like g^2 which slows the rate of convergence. Second, stacking higher Miller index planes together results not only in the layers becoming closer together but also in increasing the size of the two-dimensional-layer unit cell, hence decreasing the magnitude of the \mathbf{g} vectors. These two factors conspire to make systems such as grain boundaries and stepped surfaces computationally intractable with the usual LKKR methods and have prevented the application of conventional LEED techniques to stepped surfaces. For example, in the calculations reported below, we estimate needing *over 500* plane waves to converge the interlayer scattering. We have overcome this problem by treating scattering from neighboring layers on an angular momentum basis,¹⁴ while treating scattering from more distant layers on a plane-wave basis. In the calculations reported below, the resulting plane-wave basis is fully converged with 15 \mathbf{g} vectors. Our method shares some similarity with that recently reported by Zhang and Gonis,¹⁵ where all scattering is described in an angular momentum basis.

Turning to the problem of self-consistency, we focus upon the solution of Poisson's equation. We have developed a method for solving Poisson's equation¹⁶ using Weinert's generalized Ewald technique,¹⁷ which is appropriate for calculating self-consistent electronic structures of semi-infinite surfaces and interfaces. The solution is based upon a partitioning of the system into an unperturbed bulk region and a transition region, where the electronic structure is expected to be different from the bulk. Fourier methods are then applied in conjunction with the convolution theorem to obtain a reciprocal space representation of the charge density, and from that the potential, which can be readily implemented computationally. Although we employ the muffin-tin approximation to the potential in the calculations reported below, Weinert's method, and hence our extension, is equally applicable to full-potential calculations.¹⁸

The structure of the $\Sigma 5$ tilt boundary in nickel is shown in Fig. 1. The structure was formed by first reflecting

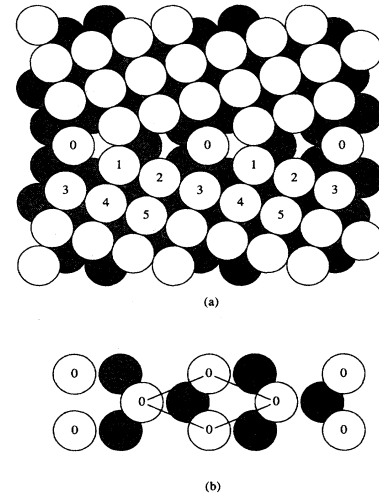


FIG. 1. (a) Structure of (210) tilt boundary, with atoms in the nearest layers labeled explicitly. (b) A plan view of the interface layer (open circles) and one of the two nearest layers (shaded circles).

semi-infinite layers of (210) planes of the face-centered-cubic (fcc) structure of Ni. The atoms in the layer labeled 1 were then relaxed to avoid overlap of muffin-tin spheres, and the atoms in the layer labeled 0 were relaxed to maximize the number of nearest neighbors. This prescription yields a similar grain-boundary structure for the nearest grain-boundary layers obtained with embedded-atom methods. The self-consistency cycle involves integrations over energy, which were performed by a sampling contour in the complex energy plane with an eight-point Gaussian quadrature scheme, and a two-dimensional Brillouin-zone average, approximated by four special \mathbf{k} points.¹⁹ The muffin-tin density of states (MTDOS) was evaluated along a contour 0.027 eV above the real energy axis with 32 \mathbf{k} points. The potentials of atoms in the layers labeled 0, . . . , 5 were allowed to relax during iteration to self-consistency, with the potentials of more distant planes of atoms taken to be that of the bulk. Thus, the interface region comprises 11 distinct atoms; as we have observed elsewhere in carrying out similar calculations for stacking faults,²⁰ a considerably larger unit cell would be required in a supercell representation to avoid interactions between adjacent faults.

The MTDOS for atoms in the vicinity of the $\Sigma 5$ grain boundary are compared with the bulk Ni MTDOS in Fig. 2. The MTDOS were obtained by integrating (1) in the region enclosed by the respective muffin-tin spheres. Calculations performed with and without empty spheres in the interstices in layer 0 produced indistinguishable MTDOS, thus providing some justification for the use of the muffin-tin approximation. The differences (e.g., reduced d -band width) are most pronounced at the interface layer (0), where the deviations from the bulk geometry in terms of coordination number and bond angles are greatest. The main peak at the Fermi energy moves to slightly lower energy, which may have consequences for the magnetization at the grain boundary and the magnetic

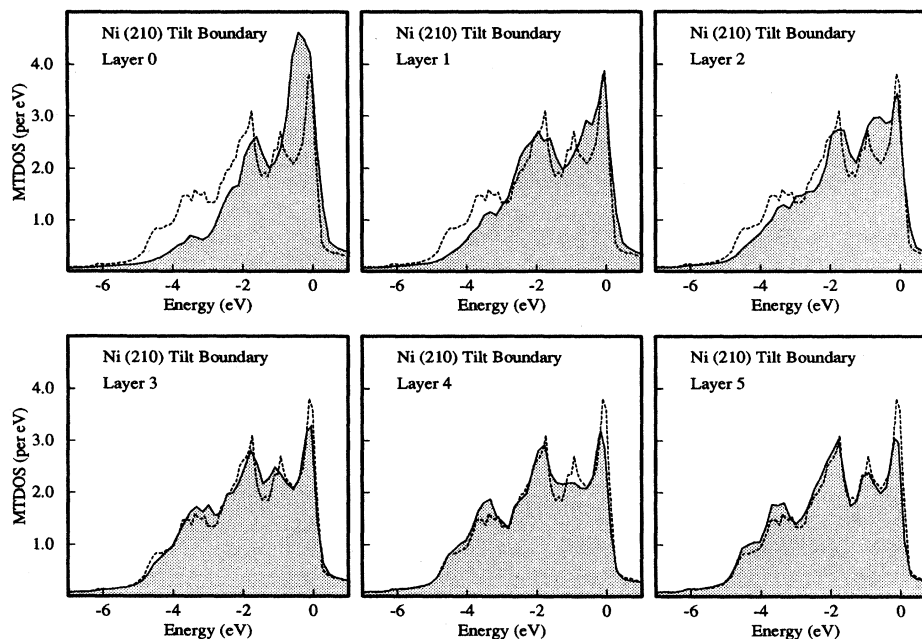


FIG. 2. MTDOS of atoms in the indicated layers near a Ni (210) tilt boundary (shaded area) compared with the MTDOS of bulk Ni (dashed lines).

contribution to the grain-boundary energy. The loss of resolution in the structure in bulk MTDOS at -1 eV (all energies quoted with respect to the Fermi energy), which is due to second-nearest-neighbor interactions (Γ_{12} -type or e_g -type states), results from the absence of the full complement of neighbors along the [100] directions. The structure resulting from nearest-neighbor interactions (Γ_{25} -type or t_{2g} -type states) at -2 eV in the bulk Ni MTDOS is, however, clearly resolved, though shifted slightly in energy. These deviations from bulk behavior clearly diminish with increasing distance from the fault, with all features restored to within $\sim 5\%$ at the third layer.

Nonmetallic impurities such as S, which have poor solubility in Ni, tend to segregate to grain boundaries, which induce brittle intergranular failure. Despite the widespread nature of embrittlement, there are many unresolved issues regarding the details of the embrittling mechanism, e.g., the role of S-S interactions and combined impurity effects. We have chosen as a first model for the $\Sigma 5$ grain boundary with S segregants a simple substitution of S for the Ni atoms in layer 0 (Fig. 1). Substitutional sites were chosen rather than interstitial sites in layer 0 because the strain caused by the relatively large size of S would make the latter relatively unstable compared to the former. The calculations of Painter and Averill⁵ support this view. Thus, a calculation with S in interstitial positions would not be realistic unless the facility to include atomic relaxations is included. In fact, the sulfided grain boundary no doubt undergoes considerable atomic rearrangement, with S present in both substitutional and interstitial positions, possibly forcing neighboring Ni into nearby interstitial sites.

The MTDOS of the sulfided $\Sigma 5$ grain boundary are

compared with those of the clean grain boundary in Fig. 3. The S MTDOS shows the effect of segregant interactions by the formation of a band between -4 and -6 eV. The effect of the segregants is seen to be largely confined to the nearest Ni layer, where there is a depletion in the Ni bonding states near -3 eV, and an overall flattening of the d bands. These features are accompanied by a significant decrease in the MTDOS at the Fermi energy, an effect also found on surfaces, where S is a well-known poison of certain types of catalytic reactions (see, e.g., Ref. 21 and references therein). The effect of S on the MTDOS of more distant layers is seen to be quite small; in particular, we find no evidence of S-induced decohesion in neighboring layers.

The origin of the depletion in the bonding states near -3 eV arises from an interference by S-S bonding *parallel* to the boundary with Ni-Ni bonding *across* the grain boundary, in part through the formation of multi-center Ni-S-Ni bonds. Note that the effect of S upon atoms in layer 3 is minimal. One effect of the S segregant is thus a local change in the elastic anisotropy, as evidenced by an increase in bonding parallel to the boundary relative to bonding perpendicular to the boundary. This enhanced anisotropy would be expected to inhibit the movement of dislocations across the grain boundary, by providing a barrier to the polarization of charge.²² The resulting pileup of dislocations near the grain boundary and the accompanying stresses could thereby provide a mechanism of S-induced intergranular fracture. To determine if there is a concomitant decohesion near the grain boundary would require detailed total-energy calculations along particular deformation paths.⁶ Studies with more dilute S concentrations are currently in progress, since reported work²³ has shown a correlation between S

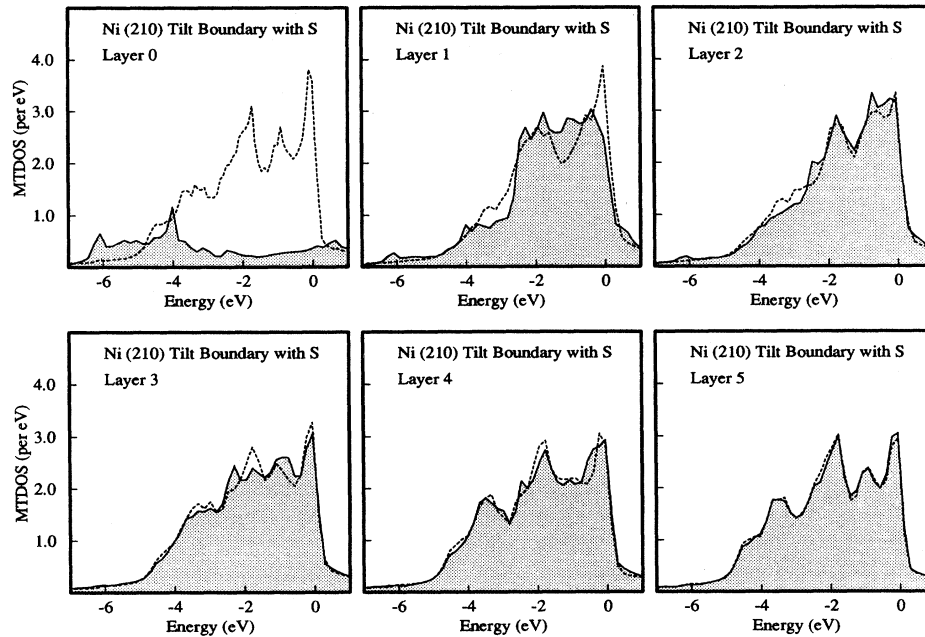


FIG. 3. MTDOS of atoms in the indicated layers near a Ni (210) tilt boundary (shaded area) with S substituted for the Ni in layer 0 compared with the associated MTDOS in Fig. 2 (dashed lines), except for the S layer, where the comparison is with the bulk Ni MTDOS (dashed line).

concentration and a tendency toward embrittlement.

To summarize, we have presented a self-consistent calculation of the electronic structure of the $\Sigma 5$ grain boundary in Ni that has the accuracy of KKR theory for bulk crystals. The efficiency of the method permits large numbers of calculations to be performed without large computing expenditures. Furthermore, removing the restriction to muffin-tin potentials²⁴ will permit not only the first-principles determination of grain-boundary energies,

but also provide accurate potentials and benchmark calculations for comparison with techniques such as the embedded-atom method.

This work was supported by the United Kingdom Science and Engineering Research Council, the Office of Naval Research, the Department of Energy, and in part by a NATO travel grant.

*Also at Department of Materials Science and Engineering, Massachusetts Institute of Technology, Cambridge, MA 02139.

¹Chemistry and Physics of Fracture, edited by R. M. Latanision and R. H. Jones (Martinus Nijhoff, Hingham, MA, 1987).

²C. L. Briant and R. P. Messmer, Philos. Mag. B **42**, 569 (1980); R. P. Messmer and C. L. Briant, Acta Metall. **30**, 457 (1982).

³M. E. Eberhart, K. H. Johnson, and R. M. Latanision, Acta Metall. **32**, 955 (1984); M. E. Eberhart, R. M. Latanision, and K. H. Johnson, *ibid.* **33**, 1769 (1985).

⁴M. E. Eberhart and D. D. Vvedensky, Phys. Rev. Lett. **58**, 61 (1987).

⁵G. S. Painter and F. W. Averill, Phys. Rev. Lett. **58**, 234 (1987).

⁶L. Goodwin, R. J. Needs, and V. Heine, Phys. Rev. Lett. **60**, 2050 (1988).

⁷M. S. Daw and M. I. Baskes, Phys. Rev. B **29**, 6443 (1984).

⁸S. P. Chen, D. J. Srolovitz, and A. F. Voter, J. Mater. Sci. **4**, 62 (1989).

⁹M. R. Fitzsimmons and S. L. Sass, Acta Metall. **37**, 1009 (1989).

¹⁰J. M. MacLaren, S. Crampin, D. D. Vvedensky, and J. B. Pen-

dry (unpublished).

¹¹F. S. Ham and B. Segall, Phys. Rev. **124**, 1786 (1961).

¹²J. B. Pendry, *Low Energy Electron Diffraction* (Academic, London, 1974).

¹³K. Kambe, Z. Naturforsch. **22a**, 422 (1967).

¹⁴J. M. MacLaren, S. Crampin, and D. D. Vvedensky (unpublished).

¹⁵X.-G. Zhang and A. Gonis, Phys. Rev. Lett. **62**, 1161 (1989).

¹⁶J. M. MacLaren, D. D. Vvedensky, and S. Crampin (unpublished).

¹⁷M. Weinert, J. Math. Phys. **22**, 2433 (1981).

¹⁸J. M. MacLaren, Bull. Am. Phys. Soc. **34**, 639 (1989).

¹⁹S. L. Cunningham, Phys. Rev. B **10**, 4988 (1974).

²⁰S. Crampin, D. D. Vvedensky, J. M. MacLaren, and M. E. Eberhart, Mater. Res. Soc. Symp. Proc. (to be published).

²¹J. M. MacLaren, D. D. Vvedensky, J. B. Pendry, and R. W. Joyner, J. Chem. Soc. Faraday Trans. **1** **83**, 1945 (1987).

²²R. Haydock, J. Phys. C **14**, 3807 (1981).

²³D. H. Lassila and H. K. Birnbaum, Acta Metall. **35**, 1815 (1987).

²⁴A. Gonis, X.-G. Zhang, and D. M. Nicholson, Phys. Rev. B **38**, 3564 (1988).